Proceedings of the 16th International Conference on Soil Mechanics and Geotechnical Engineering

doi:10.3233/978-1-61499-656-9-845

A Swinging Plane Model for soil liquefaction analysis

Un Modèle Balançant d'Avion pour l'analyse de liquéfaction de sol

S.-S. Park, P.M. Byrne & D. Wijewickreme
Department of Civil Engineering, University of British Columbia, Vancouver, Canada

ABSTRACT

A simplified constitutive model called a Swinging Plane Model is presented for monotonic and cyclic soil response including liquefaction. This model is based on two mobilized planes: a plane of maximum shear stress, which swings, and a horizontal plane which is spatially fixed. By controlling two mobilized planes, the model can simulate the principal stress rotation effect associated with simple shear from different K_0 states, which can significantly influence soil behaviour. The proposed model gives a similar skeleton behaviour for soils having the same mean stress, regardless of K_0 conditions as observed in laboratory tests. The soil skeleton behaviour observed in cyclic drained simple shear tests, including compaction during unloading and dilation at large strain is captured in the model. Undrained monotonic and cyclic response is predicted by imposing the volumetric constraint of the water on the drained or skeleton behaviour. This constitutive model is incorporated into the dynamic coupled stress-flow finite difference program FLAC (Fast Lagrangian Analysis of Continua). The model was first calibrated with drained monotonic and cyclic simple shear tests on Fraser River sand, and verified by comparing predicted and measured undrained monotonic and cyclic behaviour of Fraser River sand.

RÉSUMÉ

Un modèle constituant simplifié a appelé un Modèle d'Avion Balançant est présenté pour monotonic et la réponse de sol cyclique y compris la liquéfaction. Ce modèle est basé sur deux avions mobilisés : un avion de cisailles maximums accentue, quelles balançoires, et un avion horizontal qui est spatialement réparé. En contrôlant deux avions mobilisés, le modèle peut simuler l'effet de rotation de tension principal a associé avec les cisailles simples de différent K_0 états, qui peuvent influencer significativement du comportement de sol. Le modèle proposé donne à un comportement de squelette similaire pour les sols ayant la tension moyenne pareille, sans tenir compte de K_0 conditions comme observé dans les tests de laboratoire. Le comportement de squelette de sol a observé dans les tests de cisailles simples, drainés et cycliques, y compris le compactage pendant décharger et la dilatation à la grande tension est capturé dans le modèle. Undrained monotonic et la réponse cyclique est prédite en imposant la contrainte volumétrique de l'eau sur le comportement drainé ou de squelette. Ce modèle constituant est incorporé dans le tension-coule couplé dynamique FLAC de programme de différence fini (l'Analyse de Lagrangian Rapide de Continuum). Le modèle était premier calibré avec monotonic drainé et les tests de cisailles simples cycliques sur le sable de Rivière de Fra-ser, et vérifié en comparant prédit et mesuré undrained monotonic et le comportement cyclique de sable de Rivière de Fraser.

1 INTRODUCTION

The effect of principal stress rotation significantly influences soil behaviour and has received substantial attention since Arthur et al. (1980). A few different types of numerical models considering principal stress rotation effects have been proposed. These are mainly based on plasticity. One of them is a multilaminate model proposed by Pande and Sharma (1983). Recently, Lee and Pande (2004) presented its extension to soil liquefaction analysis. This model was originally proposed to study rock joint behavior by considering many slip planes. Alternatively, Matsuoka (1974) proposed a similar idea but a different concept called multimechanism that used only a maximum obliquity plane, $45+\phi/2$ for three different shearing mechanisms. Each shearing mechanism is based on two of three principal stresses (i.e. σ'_1 and σ'_2, σ'_2 and σ'_3, σ'_3 and σ'_1). Kabilamany and Ishihara (1991) also proposed a similar concept in three dimensional stress space. In their models, plastic strains from three mechanisms are independently produced and superimposed. The practicality of utilizing such numerical models depends on their simplicity and robustness (Kolymbas 2000). This is particularly so for dynamic analyses. Consequently, the practical application of models for dynamic analyses has been limited to few cases.

A plasticity based constitutive model has been developed at the University of British Columbia (UBC) to handle plastic unloading and principal stress rotation associated with anisotropic consolidation, or K_0 state and is presented here. The proposed model uses two mobilized planes, a maximum shear stress plane which rotates or swings with as the direction of the principal stress rotates, and a horizontal plane which is spatially fixed. Under simple shear conditions the plane of maximum shear is initially at 45 degrees to the horizontal and as the shear stress is applied the plane swings and becomes nearly horizontal at failure. This concept is therefore referred to as a Swinging Plane Model. The characteristics of this model and its formulation are introduced, and a comparison with laboratory data is presented.

2 SIMPLE SHEAR BEHAVIOUR UNDER ISOTROPIC AND K_0 CONDITIONS AND ITS MODELLING

Rotation of principal stresses occurs in simple shear loading and its effect depends very much on the initial K_0 consolidation state. If $K_0 = 1.0$, then as soon as any horizontal shear stress is applied, the horizontal plane become the plane of maximum shear and essentially remains so for the rest of the loading. For this case the plane of maximum shear is horizontal for the duration of loading, and there is no rotation effect. Classical plasticity with a single rotating plane of maximum shear simulates this condition very well. If $K_0 = 0.5$, then a large shear stress acts on the 45 degree plane. As the horizontal shear stress is applied, the plane of maximum shear gradually rotates and becomes

approximately horizontal at failure (Roscoe 1970). Thus, there is a gradual rotation of principal stress during the loading process. A classical plasticity approach with a single plane cannot capture the observed response in this case. We have found that the observed response can be captured by adding a plastic contribution from the horizontal plane.

From drained monotonic torsional tests using hollow cylindrical samples, Wijewickreme and Vaid (2004) found that the shear stress-shear strain behaviour on a horizontal plane under the same mean stress is independent of stress path at small strain ranges (shear strain $\gamma < 0.5$ %) for loose sand. In simple shear, this finding can infer that shear stress-strain behaviour of loose sands is the same at small strain level regardless of K_0 state as long as initial mean stresses are the same.

Ishihara (1996) showed that K_0 has a significant effect on liquefaction resistance of sands based on a series of torsional tests with lateral confinement. He found that the cyclic resistance ratio, τ/σ_{v0}' where σ_{v0}' is the initial vertical effective stress, under $K_0 = 1.0$ condition is stiffer and stronger than that observed under $K_0 = 0.5$ condition. On the other hand, there was no significant difference between the $K_0 = 1.0$ and 0.5 conditions when the cyclic resistance was examined in terms of τ/σ_{m0}' where σ_{m0}' is the initial mean effective stress. Iai et al. (1992) considered K_0 consolidated elements using a generalized plasticity approach. They mentioned that conventional plasticity models cannot simulate $K_0 = 0.5$ simple shear tests because they involve effects of rotation of principal stress. The proposed plasticity model can simulate rotation effects associated with K_0 simple shear loading by incorporating two mobilized planes rather than one. Numerical simulations under two K_0 conditions, 0.5 and 1.0, are compared with measured liquefaction behaviour.

The proposed model referred to as a Swinging Plane Model is an extension of a simpler model called UBCSAND to include plastic unloading and rotation of principal planes associated with simple shear loading. UBCSAND originally considered unloading as elastic. From a practical point of view, elastic unloading may be adequate for preliminary analysis. However, laboratory data indicate that significant plastic deformation always occurs during the unloading phase. Plastic unloading is particularly important following a large stress cycle that has induced dilation. In the proposed constitutive model, plastic unloading is incorporated by mobilizing plastic deformation on a horizontal plane.

3 SWINGING PLANE MODEL

The UBCSAND modifies the Mohr-Coulomb model incorporated in FLAC (Fast Lagrangian Analysis of Continua) Version 4.0 (Itasca 2000) to incorporate the plastic strains that occur at all stages of loading. This model has been substantially improved to better model observed sand behaviour and include the effects of rotation of principal planes or K_0 effect, and plastic unloading as mentioned earlier. These two factors recently incorporated into the Swinging Plane Model are presented in this paper. The concept and formulations of this model are described in this section including plastic deformations mobilized on two planes.

3.1 *Concept of Swinging Plane Model*

The concept of Swinging Plane Model is described here. Shear stress increments on two planes causing plastic strains are illustrated in Figure 1 for simple shear conditions with $K_0 = 0.5$. Figure 1(a) represents conditions at the start of shearing when $\tau_{xy} = 0$ and a small increment $\Delta\tau_{xy}$ is applied. In this case the plane of maximum shear is at 45 degrees ($\beta = 45°$) as illustrated in Figures 1(a) and 2(a), and while there is a large shear stress from the K_0 condition, the increments of shear and normal stresses $\Delta\tau$ and $\Delta\sigma$ on this plane are both zero, and hence no plastic strains are predicted. This results in an initial very stiff elastic response from classical plasticity based on a single plane. However, the stress increment on the horizontal plane, $\Delta\tau_{xy}$ will cause plastic strains on the horizontal plane and all other planes except for the 45 plane. When this second plane is considered, a much softer response is predicted as shown in Figure 3, condition A.

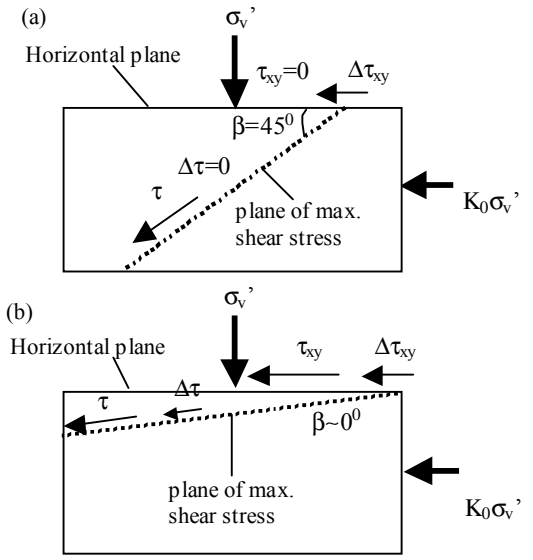

Figure 1. Stress conditions on two mobilized planes: (a) at small strain level and (b) at large strain level

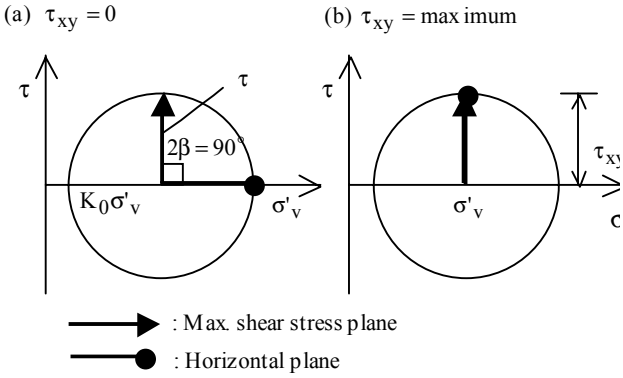

Figure 2. Swinging of the plane of maximum shear stress under K_0 condition

A later stage of loading is depicted in Figure 1(b). Here τ_{xy} is approaching its failure value and the plane of maximum shear has swung around to become nearly horizontal as illustrated in Figures 1(b) and 2(b). Now the $\Delta\tau \approx \Delta\tau_{xy}$ and both planes essentially coincide. Consideration of both planes would essentially predict double the plastic strain. This is accounted for by gradually phasing out the plastic strain increment from the horizontal plane as the plane of maximum shear becomes horizontal. This stress strain condition is depicted as condition B on Figure 3. Note that if $K_0 = 1$ then the plane of maximum shear becomes horizontal as soon as the first increment of $\Delta\tau_{xy}$ is applied and the horizontal plane contribution is not needed. It is depicted in Figure 2(b).

In summary, for simple shear conditions, the predicted response from classical plasticity will be too stiff if only the plane of maximum shear is considered as depicted in Figure 3. By including the plastic strain increments from the horizontal plane a softer response in keeping with observed response is predicted. For the special case of $K_0 = 1$, the plane of maximum shear is approximately horizontal throughout simple shear loading, and there is no need to consider a second plane. For cyclic triaxial tests the direction of principle stress remains vertical and there is no rotation of principle stress and no need to consider a second plane. However, earthquakes induced loading conditions are much closer to simple shear than conventional triaxial loading, and it is important therefore to consider a second plane for seismic loading.

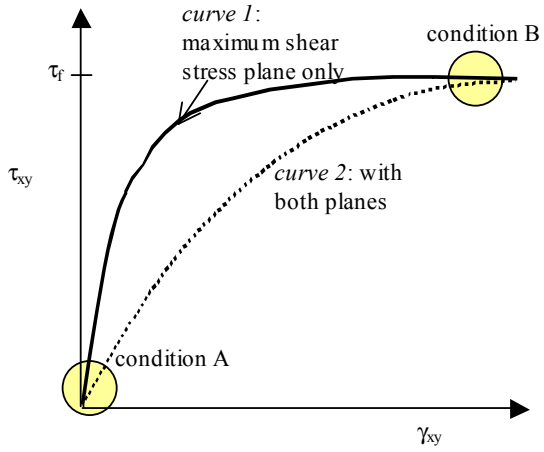

Figure 3. Shear stress-strain curves using two mobilized planes under K_0 condition

3.2 *Elastic behaviour*

Elastic behaviour is assumed isotropic and expressed in terms of bulk and shear moduli. The elastic bulk modulus, B, and shear modulus, G, are stress level dependent and described by the following relations, where K_B^e and K_G^e are modulus numbers, P_A is atmospheric pressure, and σ'_m is the mean effective stress:

$$B = K_B^e \cdot P_A \cdot \left(\frac{\sigma'_m}{P_A} \right)^{0.5} \quad (1)$$

$$G = K_G^e \cdot P_A \cdot \left(\frac{\sigma'_m}{P_A} \right)^{0.5} \quad (2)$$

3.3 *Plastic behaviour on maximum shear stress plane*

The formulation is based on classical plasticity. Yield loci are radial lines from the origin of stress space corresponding to the mobilized friction angle. The proposed model is a Mohr-Coulomb type of model (Vermeer 1980). Since the sine of a mobilized friction angle corresponds to the ratio of shear stress to mean stress, τ/σ'_m, yield loci f_1 are assumed to be radial lines of constant stress ratio as shown in Figure 4 and expressed by

$$f_1 = \tau_1 - \sigma'_m \cdot \sin(\phi_{mob})_1 \quad (3)$$

where τ_1 = the maximum shear stress, and $(\phi_{mob})_1$ = the friction angle mobilized on the maximum shear stress plane. Reloading induces plastic response but with a stiffened plastic shear modulus. The plastic shear modulus relates the shear stress and the plastic shear strain and is assumed to be hyperbolic with stress ratio as shown in Figure 5. Moving the yield locus from A to B in Figure 4 induces a plastic shear strain increment, $d\gamma^P$, as shown in Figure 5, and is controlled by the plastic shear modulus, G^P. The flow rule defines the direction of the plastic strain increments and is non-associated here. The plastic potential g_1 used in the flow rule is a function of dilation angle as follows:

$$g_1 = \tau_1 - \sigma'_m \cdot \sin(\psi)_1 \quad (4)$$

where $(\psi)_1$ is the dilation angle based on laboratory data and energy considerations and is approximated by

$$\sin(\psi)_1 = \sin\phi_{cv} - \sin(\phi_{mob})_1 \quad (5)$$

where ϕ_{cv} is the phase transformation or constant volume friction angle and $(\phi_{mob})_1$ describes the current yield locus. A positive value of $\sin(\psi)_1$ corresponds to contraction. Contraction occurs for stress states below ϕ_{cv} and dilation above. The associated plastic volumetric strain increment, $d\varepsilon_v^P$, is obtained from $d\gamma^p$ and the dilation angle $(\psi)_1$:

$$d\varepsilon_v^P = d\gamma^P \cdot \sin(\psi)_1 \quad (6)$$

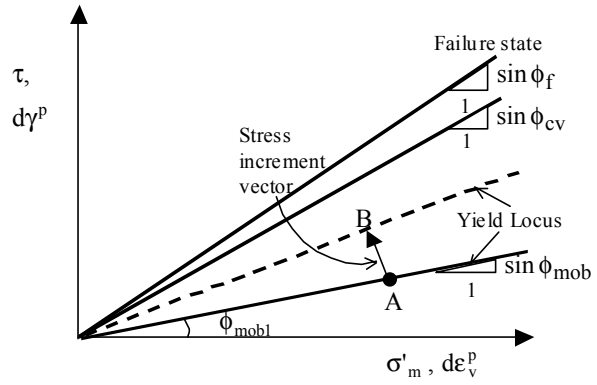

Figure 4. Failure and yield conditions

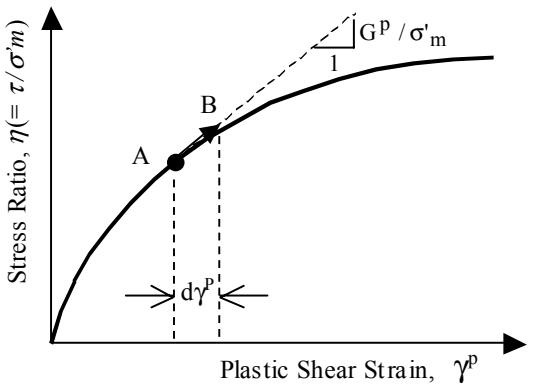

Figure 5. Hardening rule

3.4 *Plastic behaviour on horizontal plane*

Yield loci associated with the horizontal plane, f_2, have the same shape as those for the maximum shear stress plane and are expressed by

$$f_2 = \tau_2 - \sigma'_m \cdot \sin(\phi_{mob})_2 \tag{7}$$

where $\tau_2 = \tau_{xy}$, the shear stress acting on a horizontal plane, and $(\phi_{mob})_2$ = the friction angle mobilized on a horizontal plane. The horizontal plane will contribute to both loading and unloading component. In terms of the amount of plastic strains, this contribution will be maximum when shearing starts under a K_0 state. It will gradually decrease as the plane of maximum shear stress rotates. After the maximum shear stress plane becomes horizontal, the contribution from this horizontal plane becomes zero. The plastic volumetric strain increment and dilation angle are similar to those in Eq. 5 and Eq. 6. However, the dilation angle, sin $(\psi)_2$, is based on a mobilized angle on a horizontal plane, sin $(\phi_{mob})_2$ and expressed by

$$\sin(\psi)_2 = \sin\phi_{cv} - \sin(\phi_{mob})_2 \tag{8}$$

3.5 *Hardening rule and elasto-plastic behaviour*

The hardening rules are similar for both maximum shear stress and horizontal planes. The only difference is the stress ratio, η. The plastic properties used by the model are the peak friction angle ϕ_P, the constant volume friction angle ϕ_{cv}, and plastic shear modulus G^P, where

$$G^P = G_i^P \cdot \left(1 - \frac{\eta}{\eta_f} R_f\right)^2 \tag{9}$$

$G_i^P = \alpha G$ and α depends on relative density, η (= τ_1/σ'_m or τ_2/σ'_m) is the stress ratio, η_f is the stress ratio at failure, and R_f is the failure ratio used to truncate the hyperbolic relationship.

For loading on the plane of maximum shear, the position of the yield locus $(\phi_{mob})_1$ is initially specified for each element. As the stress ratio increases and plastic strain is predicted, the yield locus for that element is pushed up by an amount $d(\phi_{mob})_1$ as given by Eq. 10.

$$d(\phi_{mob})_1 = \left(\frac{G^P}{\sigma'_m}\right) \cdot d\gamma^P \tag{10}$$

Upon unloading, plastic deformation is controlled by conditions on the horizontal plane using an incremental formulation of Eq. 7 and expressed in Eq. 11. The initial yield locus is set at the stress reversal point C in Figure 6 and plastic shear strain, $d\gamma^p$, upon unloading is predicted based on Eq. 11 until the shear stress changes sign, or reversal occurs.

$$df_2 = d\tau_2 - d\sigma'_m \cdot \sin(\phi_{mob})_2 - G^p \cdot d\gamma^p = 0 \tag{11}$$

During unloading and reloading, plastic shear moduli are based on modified shear stresses as given by Eq. 12 and illustrated in Figure 6, where $\eta^* = \tau^*/\sigma'_m$ and $\eta_f^* = \tau_f^*/\sigma'_m = (\tau_r+\tau_f)/\sigma'_m$. Reloading then occurs with a stiffened modulus:

$$G^P = G_i^P \cdot \left(1 - \frac{\eta^*}{\eta_f^*} R_f\right)^2 \tag{12}$$

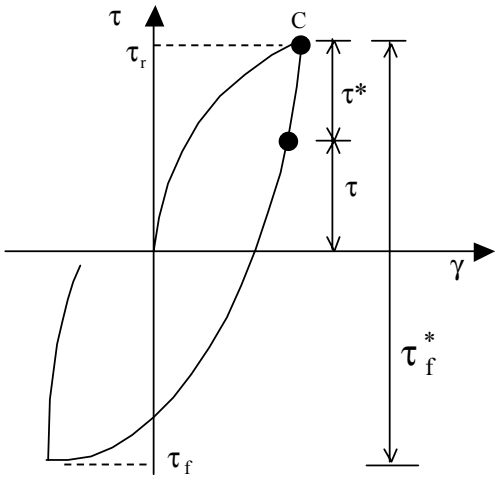

Figure 6. Stress ratio during unloading and reloading

The plastic volumetric strain increment is obtained from Eqs. 13 and 14 through dilation angle, sin $(\psi)_2$. Eq. 13 is for loading and Eq. 14 is for unloading as illustrated in Figure 7. These equations are based on stress-dilatancy theory as well as the results of drained cyclic simple shear tests, Lee (1991). His results showed that dilation angle depended on stress ratio, η, and whether loading or unloading is occurring, but was not influenced by the initial density, normal stress, or number of cycles.

$$\frac{d\varepsilon_v^p}{|d\gamma^p|} = (\sin\phi_{cv} - \eta) = \sin(\psi)_2 \tag{13}$$

$$\frac{d\varepsilon_v^p}{|d\gamma^p|} = (\sin\phi_{cv} + \eta) = \sin(\psi)_2 \tag{14}$$

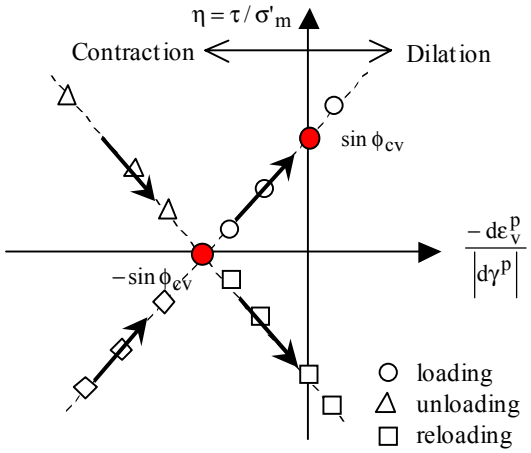

Figure 7. Shear volume coupling

Plastic shear and volumetric strain increments from both the plane of maximum shear and the horizontal plane are simply added as shown in Eq. 15.

$$\left(d\varepsilon^{p}\right)_{k} = \lambda_{k} \cdot \frac{\partial g_{k}}{\partial \sigma} \qquad (15)$$

where k indicates each mobilized plane causing plastic deformation (i.e. k = 1,2), λ is a scalar number, and determined by a consistency condition (i.e. df = 0). Plastic strain increments resulting from principal stress rotation during both loading and reloading are considered on the horizontal plane. Their contribution gradually decreases as principal stresses rotate and becomes zero when both planes are coincident. A scalar number λ_2 on a horizontal plane is adjusted to λ_2* as follows

$$\lambda_2^* = \lambda_2 \cdot (\cos 2\alpha_\sigma)^\chi \text{ , where } 0 \le (\cos 2\alpha_\sigma)^\chi \le 1.0 \qquad (16)$$

where α_σ is a principal stress rotation angle from the vertical, and χ is an adjusting parameter to give a best fit. When both planes are coincident, $\lambda_2^* = 0$.

The response of sand is controlled by the skeleton behaviour. A fluid (air water mix) in the pores of the sand acts as a volumetric constraint on the skeleton if drainage is curtailed. It is this constraint that causes the pore pressure rise that can lead to liquefaction. Provided the skeleton or drained behaviour is appropriately modeled under monotonic and cyclic loading conditions, and the stiffness of the pore fluid (B_f) and drainage are accounted for, the liquefaction response can be predicted. This concept is incorporated in the Swinging Plane Model.

4 CALIBRATION

A series of simple shear tests were performed on Fraser River sand at UBC and used as a database to calibrate the numerical model element response. Test data are available on web site (http://www.civil.ubc.ca/liquefaction/). The samples were prepared by air pluviation method, which is normally adopted in centrifuge tests. The details including test results can be found in Wijewickreme et al. (2005) and Sriskandakumar (2004). Drained behaviour of the sand was first captured by the model as shown in Figure 8.

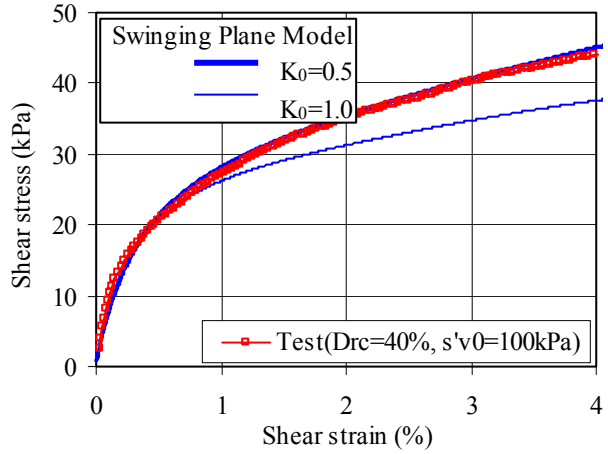

Figure 8. Numerical simulations of K_0 =0.5 and 1.0 with the same initial mean stress

Two numerical predictions with the same initial mean stress for the test (D_{rc} = 40 % and σ'_{v0} = 100 kPa) give similar response at small shear strain (γ < 1 %), regardless of K_0 conditions. Upon further shearing, the K_0 = 0.5 case (thick line) gives a stiffer response because the horizontal stress rises and increases σ'_m.

Samples were also subjected to cyclic shear for a range of cyclic stress ratios under constant volume conditions that simulate undrained response. Tests were carried out for four different CSRs (Cyclic Stress Ratio), 0.08, 0.1, 0.12 and 0.15. Typical results of measured response of D_{rc} = 40 % for CSR = 0.1 are shown in Figures 9a and 9b. Test data are shown as the heavy lines. The thin lines are the numerical predictions for K_0 = 0.5. When CSR = 0.1, liquefaction occurred in 6 cycles. It is observed that the first and last cycles generated large excess pore pressures. Once the pore pressure ratio reached unity, large cyclic strains developed referred to as cyclic mobility.

The CSR versus number of cycles to liquefaction is shown in Figure 10. Liquefaction triggering was defined as γ > 3.75 %, and at this point R_u (pore pressure ratio) is 90 - 95 %. This strain level is equivalent to reaching a 2.5% single-amplitude axial strain in a triaxial sample, which also is a definition for liquefaction previously suggested by the National Research Council of United States (NRC 1985).

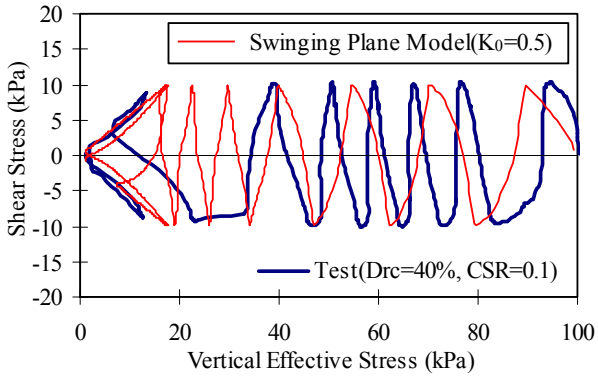

Figure 9a. Predicted stress path under K_0 = 0.5 and test result

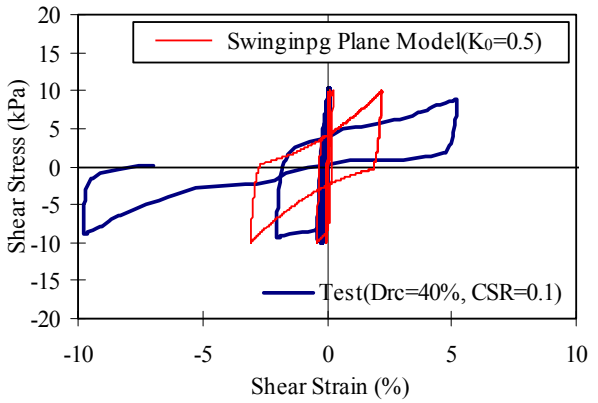

Figure 9b. Predicted stress-strain curve under K_0 = 0.5 and test result

The calibration was carried out in the same way as the tests, i.e. under constant volume. The test sample was subjected to an initial vertical stress of 100 kPa under K_0 conditions. It was assumed that the initial horizontal stress in the test was 50 kPa, i.e., K_0 = 0.5. The same initial stresses were assumed in the numerical simulation. A single element was used. The elastic and plastic parameters selected for calibration were the same for all cases having the same D_r and tabulated in Table 1. The predicted stress-strain and stress paths for K_0 = 0.5 and CSR = 0.1 are shown in Figures 9a and 9b as "thin" lines. The predictions generally give a reasonable representation of the observed response including plastic unloading, sudden drop of effective stress during stress reversal after dilation, and cyclic mobility.

Table 1. Input parameters for Drc = 40 % Fraser River sand

Parameters	K_G^e	$K_B e$	α	ϕ_{cv}	η_f	R_f
Values	622	249	0.4	33	0.58	0.99

If test condition were K_0 = 0.5, the predicted triggering of liquefaction shows a good agreement with measurements as shown in Figure 10.

An examination of the effect of K_0 on prediction of liquefaction resistance is shown in Figure 11. The K_0 = 0.5 case had initial stresses of 100 kPa and 50 kPa, and thus a mean stress of 75 kPa. The K_0 = 1.0 case had stresses of 75 kPa, and thus a mean stress of 75 kPa also. The predicted results show that both K_0 = 0.5 and K_0 = 1.0 states liquefaction in about the same number of cycles. This is in agreement with the test results of Ishihara (1996) who found that samples at the same density and mean stress had similar liquefaction response.

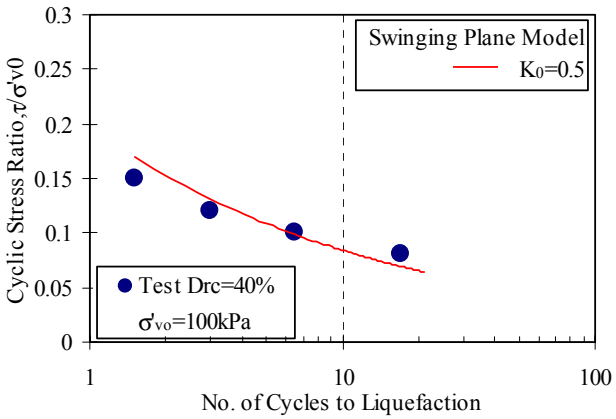

Figure 10. Predicted liquefaction resistance under K_0 = 0.5 and test result in terms of τ/σ'_{v0}

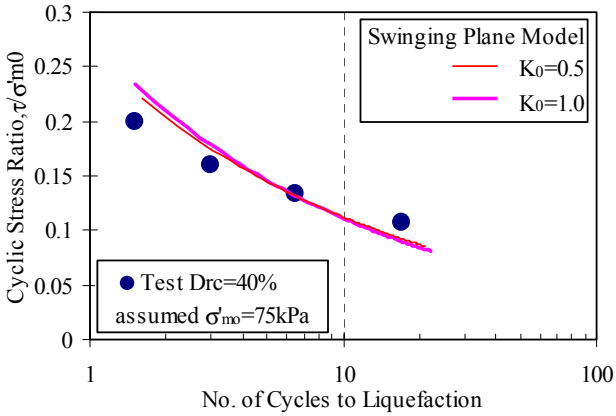

Figure 11. Predicted liquefaction resistance in terms of τ/σ'_{m0} under K_0 = 0.5 and 1.0 and test result

5 CONCLUSION

A Swinging Plane Model for predicting the stress-strain response of sand under monotonic as well as cyclic loading conditions is presented. The model is focused on simple shear loading conditions, as this is most representative of seismic loading conditions in the field. The proposed model addressed two key features; rotation of principal planes and plastic unloading. It uses two mobilized planes; a maximum shear stress plane, and a horizontal plane. The model was calibrated based on drained and constant volume simple shear tests and showed the same characteristic response as observed in the laboratory tests. The model captured the large soil compaction effect during stress reversal after dilation and general cyclic soil behaviour including cyclic mobility after triggering of liquefaction. The model also predicts that elements having the same initial density and mean stress will have similar liquefaction response, in agreement with laboratory element tests.

ACKNOWLEDGMENTS

Authors acknowledge that a series of simple shear tests for numerical model validation presented herein were carried out by Mr. Sriskandakumar during his MASc studies at the University of British Columbia under the supervision of Dr. Wijewickreme at UBC. The authors also acknowledge NSERC support through grant No. 246394, without which this work would not have been possible.

REFERENCES

Arthur, J. R. F., Chua, K. S., Dunstan, T. and Rodriguez del C. J. I. 1980. Principal stress rotation: a missing parameter. *Journal of the Geotechnical Engineering Division*, 106(GT4), 419-433

Iai, S., Matsunaga, Y., and Kameoka, T. 1992. Analysis of undrained cyclic behavior of sand under anisotropic consolidation. *Soils and Foundations*, 32(2), 16-20.

Ishihara, K. 1996. *Soil behaviour in earthquake Geotechnics*. Clarendon Press, Oxford.

Itasca. 2000. FLAC, version 4.0. Itasca Consulting Group Inc., Minneapolis.

Kabilamany, K., and Ishihara, K. 1991. Cyclic behaviour of sand by the multiple shear mechanism model. *Soil Dynamics and Earthquake Engineering*, 10(2), 74-83.

Kolymbas, D. 2000. The misery of constitutive modelling. *Constitutive modelling of granular materials*. Edited by Dimitrios Kolymbas: 11-24.

Lee, C.- J. 1991. Deformation of sand under cyclic simple shear loading. Proceedings of the Second International Conference on Recent Advances in Geotechnical Earthquake Engineering and Soil Dynamics, March 11-15, St. Louis, Missouri, 1, 33-36.

Lee, K.-H. and Pande, G. N. 2004. Development of a two-surface model in the Multilaminate framework. Proceedings of the 11th Conference on Numerical Models in Geomechanics, Ottawa, pp. 139-144.

Matsuoka, H. 1974. Stress-strain relationships of sands based on the mobilized plane. *Soils and Foundations*, 14(2), 47-61.

NRC. 1985. Liquefaction of soils during earthquakes. National Research Council Report CETS-EE-001, National Academic Press, Washington, D.C.

Pande, G. N., and Sharma, K. G. 1983. Multi-laminate model of clays-a numerical evaluation of the influence of rotation of the principal stress axes. *Int. Journal for Numerical and Analytical Methods in Geomechanics*, 7, 397-418.

Roscoe, K.H. 1970. 10th Rankine Lecture: The influence of strains in soil mechanics. *Geotechnique*, 20: 129-170.

Sriskandakumar, S. 2004. Cyclic loading response of Fraser River sand for validation of numerical models simulating centrifuge tests. MASc Thesis, Department of Civil Engineering, UBC.

Vermeer, P. A. 1980. Formulation and analysis of sand deformation problems." Report 195 of the Geotechnical Laboratory, 142p. Delft University of Technology.

Wijewickreme, D. and Vaid, Y. P. 2004. A descriptive framework for the drained response of sands under simultaneous increase in stress ratio and rotation of principal stresses. Submitted to *Soils and Foundations*.

Wijewickreme, D., Sriskandakumar, S., and Byrne, P.M. 2005. Cyclic Loading Response of Loose Air-pluviated Fraser River Sand for Validation of Numerical Models Simulating Centrifuge Tests, *Canadian Geotechnical Journal* (in print).